

## Natural fiber substitution in glass fiber-reinforced plastics: A Tensile properties simulation

Alief Wikarta<sup>1\*</sup>, Chandya Andikusuma<sup>1</sup>, Julendra Bambang Ariatedja<sup>1</sup>, I Made Londen Batan<sup>1</sup>, Femiana Gapsari<sup>2</sup> and Sze Wei Khoo<sup>3</sup>


<sup>1</sup> Department of Mechanical Engineering, Faculty of Industrial Technology and Systems Engineering, Institut Teknologi Sepuluh Nopember, **Indonesia**

<sup>2</sup> Department of Mechanical Engineering, Faculty of Engineering, Universitas Brawijaya, **Indonesia**

<sup>3</sup> Department of Industrial Engineering, Universiti Tunku Abdul Rahman, **Malaysia**

\* Corresponding Author: [wikarta@me.its.ac.id](mailto:wikarta@me.its.ac.id)

*Received:* 26 January 2025; *Revised:* 04 June 2025; *Accepted:* 07 June 2025

 **Cite this** <https://doi.org/10.24036/teknomekanik.v8i1.33472>

**Abstract:** Glass fiber-reinforced polymer composite materials, commonly used for industrial axial flow fan blades due to their high strength-to-weight ratio, are environmentally criticized for their non-biodegradability. This concern has prompted the investigation of eco-friendly alternatives, such as sisal and kenaf as natural fibers. Although they generally have lower mechanical properties than synthetic fibers, they offer advantages in terms of biodegradability, cost, and density. This study aims to evaluate the feasibility of partially substituting glass fiber with unidirectional natural fibers kenaf and sisal in a 14-layer GFRP axial fan blade through numerical simulation. The research employed a finite element method (FEM) to simulate tensile testing in accordance with ASTM D-638 standards. Several hybrid layer configurations were analyzed, focusing on the number and position of natural fiber layers replacing glass fiber, particularly the glass roving (GR) layers. The simulation investigated how these substitutions influence the overall tensile stress and elastic modulus of the composite blade structure. The findings suggest that this substitution does not significantly affect tensile characteristics but substantially improves the biodegradability of the composite, resulting in a more environmentally friendly material without compromising mechanical performance.

**Keywords:** finite element analysis; GFRP; hybrid composite; natural fiber; tensile test

### 1. Introduction

Composite materials are materials composed of two or more different substances, where the properties of the individual components remain distinct [1]. Composites are primarily made up of two main constituents: the matrix and the reinforcement. The primary advantage of composite materials lies in their unique combination of high strength and low weight, which is unattainable with conventional materials like metals. One widely used type of composite material is glass-fiber reinforced polymer (GFRP). GFRP materials are commonly applied in ship hulls, infrastructure, military equipment, electronic devices, etc. However, over time, the waste generated by GFRP has increasingly polluted the environment because GFRP is challenging to recycle [2]. Numerous studies have been conducted on GFRP through simulations, such as the application of GFRP in turbine blades [3], the use of GFRP in bridge decks [4], and studied GFRP in bumper beams [5]. This issue aligns with Sustainable Development Goal (SDG) 12, as recent studies have demonstrated biodegradable and environmentally friendly alternatives for sustainable composite materials [6], [7].

Recently, there has been growing awareness of the importance of using environmentally friendly materials. Industries are actively seeking ways to reduce the carbon footprint and environmental impact of the materials they use. One potential solution is to replace synthetic fibers with natural fibers [8], [9], [10]. Natural fibers offer several advantages over synthetic fibers, including being biodegradable [11], having lower cost [12] and lower density [13]. However, natural fibers also have some drawbacks. The quality of natural fibers can vary depending on growing conditions, processing, and the source of the raw materials, which can affect the consistency of composite material performance [11]. Generally, natural fibers have lower mechanical properties than synthetic fibers, such as glass fibers, which can limit their use in applications requiring high strength. Additionally, natural fibers tend to be more susceptible to moisture and other environmental conditions, which can affect the stability and longevity of composite materials [14]. Therefore, natural fibers cannot yet fully replace synthetic fibers. This topic is highly interesting and has been widely researched, with studies focusing on various natural fibers such as bamboo [15], hemp and flax fibers [16], sisal and kenaf fibers [17], and banana fibers [18]. In response, this study aims to evaluate the feasibility of partially substituting glass fiber with unidirectional natural fibers kenaf and sisal in a 14-layer GFRP axial fan blade through numerical simulation.

Hybrid composites are used to combine the strength and stiffness of synthetic fibers with the sustainability and biodegradability of natural fibers. These composites consist of two or more different types of fibers or reinforcements [19]. One study demonstrated that incorporating woven bamboo layers into fiberglass composites increased tensile strength from 98 MPa to over 221 MPa, exceeding the Indonesian Classification Bureau (BKI) standard of 98 MPa for 10GT-sized ships [20]. Additionally, the addition of pine tree leaf (PTL) fillers and double layers of E-glass reinforcement in epoxy composites improved tensile strength from 32 MPa (PTL only) to 156 MPa, compressive strength to 29 MPa, and flexural strength to 220 MPa [21]. Thus, hybrid composites offer an efficient and effective solution for various applications, including in the construction, transportation, and sports equipment industries.

A study investigated a fan blade made up of 14 layers of glass fibers in various forms, including woven roving (WR), glass roving (GR), unidirectional glass, and chopped strand mat (CSM) introduced the concept of a hybrid composite by replacing GR with woven jute [2]. However, the results showed that woven jute was not a sufficient replacement for the original glass fiber material. Hence, the present study explores the use of alternative natural fibers, specifically unidirectional kenaf and sisal, to replace GR in the same fan blade configuration. These natural fibers are more environmentally friendly and have promising mechanical characteristics [22]. Unlike previous studies, this research is the first to utilize finite element simulation to systematically investigate the layer-wise substitution of GR with kenaf and sisal fibers in a GFRP fan blade. The objective is to identify the optimal hybrid composite configuration, maintaining tensile strength while increasing the natural fiber content, thereby offering a pathway to more sustainable composite applications in industrial components.

## 2. Material and methods

### 2.1 Material

In this study, the GFRP material configuration was adapted from the previous study [2], which involved a fan blade composed of various forms of glass fibers, such as woven roving (WR) 360 GSM, glass roving (GR) 280 GSM, unidirectional glass 1200 GSM (UD), and chopped strand mat (CSM) 450 GSM, with the arrangement  $[CSM/(GR/WR)_4/G/(WR/GR)_2]$ , as shown in Figure 1.



**Figure 1.** Stack up Sequence of GFRP fan blade material  $[CSM/(GR/WR)_4/G/(WR/GR)_2]$

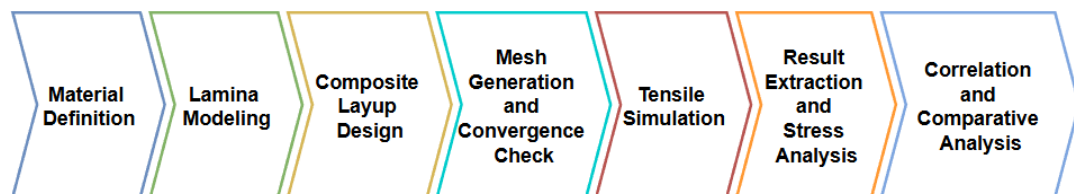
Kenaf and sisal fibers were chosen based on positive results found in several studies. According to material properties, Kenaf fiber exhibits superior tensile strength, making it a potential candidate for use as reinforcement in composite materials. Meanwhile, sisal fiber is known for its weather-resistant characteristics [23], which are crucial for fan blades. Additionally, sisal fiber has been widely used in traditional applications for many years, demonstrating its proven quality. The mechanical properties of the fibers and matrix used in this study can be found in Table 1.

**Table 1.** Mechanical Properties of the Reinforcement and Matrix

	Density (g/cm <sup>3</sup> )	Young's Modulus (GPa)	Poisson's Ratio	Shear Modulus (Gpa)	Reference
Glass	2.54	70.8	0.22	29.02	[2]
Sisal	1.5	23.5	0.32	8.9	[16], [24]
Kenaf	1.45	53	0.324	20.02	[24], [25]
Epoxy	1.14	3.4	0.35	1.26	[2]

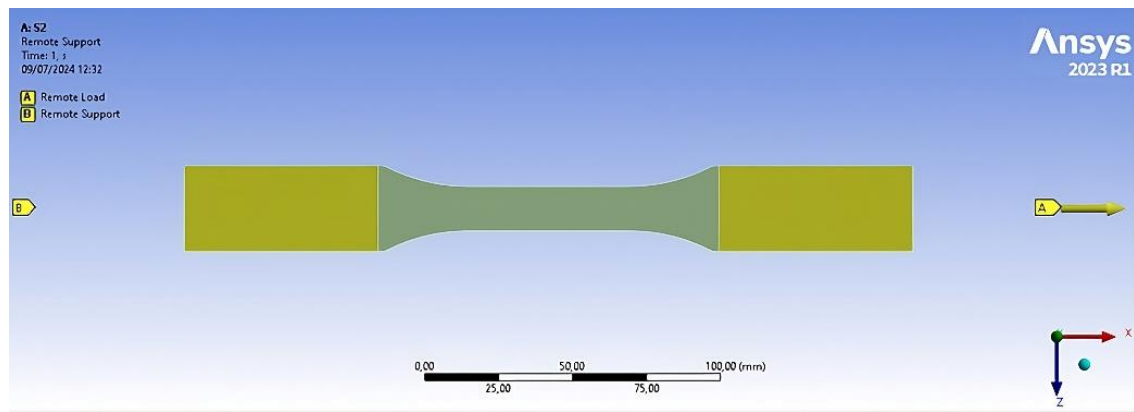
## 2.2 Simulation procedure

Figure 2 illustrates the stepwise simulation workflow conducted in this study to evaluate the tensile performance of hybrid composite materials. The simulation process started by creating a combined matrix and reinforcement model using Material Designer to determine the mechanical properties of the lamina. Each lamina had a thickness of 1 mm, a fiber volume fraction of 55%, and a fiber orientation angle of 0°. These properties were then used to configure the GFRP material arrangement in Ansys Composite PrepPost (ACP). Subsequently, a tensile test simulation was carried out using Static Structural. All simulations were performed using ANSYS software under a valid academic license provided by Institut Teknologi Sepuluh Nopember (ITS).



**Figure 2.** Stepwise simulation workflow for hybrid composite tensile analysis

The tensile test specimen used was shaped like a dog-bone according to ASTM D638. For the boundary condition, two remote displacements were applied (Figure 3). One remote displacement was placed on one side of the specimen to act as a support, while another side had a remote displacement acting as a load with a displacement magnitude of 1.90872 mm. This displacement corresponds to the maximum displacement of the GFRP material at failure [2]. This displacement value was applied uniformly across all material configurations to ensure comparability of the simulation results.



**Figure 3.** Boundary condition of tensile test in finite element analysis

In this study, two different composite material models were used as shown in Figure 4. The main difference between these two models was the material used in the 10th layer. In Model 1, UD glass was used in the 10th layer, which represented the conventional configuration for GFRP material in fan blades. On the other hand, in Model 2, UD glass in the 10th layer was replaced with UD kenaf. The choice of UD kenaf as a substitute was based on its superior stiffness and better biodegradability compared to UD glass. In each model, the Glass Roving (GR) in the 2nd, 4th, 6th, 8th, and 12th layers were replaced with UD kenaf and UD sisal (Table 2 - Table 5). This replacement aimed to increase the proportion of natural fibers in the GFRP fan blade material. This change is expected to maintain or even enhance the mechanical properties of the composite material while improving sustainability using natural fibers.

This study employed a series of analytical methods to evaluate the mechanical properties of the composite material. Tensile test simulations were firstly conducted to determine the tensile properties, including maximum stress and Young's Modulus, for each configuration. The results were then analyzed to evaluate the effects of replacing glass fibers with natural fibers across different configurations. A stress distribution analysis was subsequently performed to investigate how stress was distributed across individual layers of the composite, providing insights into the localized mechanical behavior of each layer. Additionally, a correlation analysis was carried out to evaluate the relationship between the position of replaced glass fibers and the resulting tensile properties.

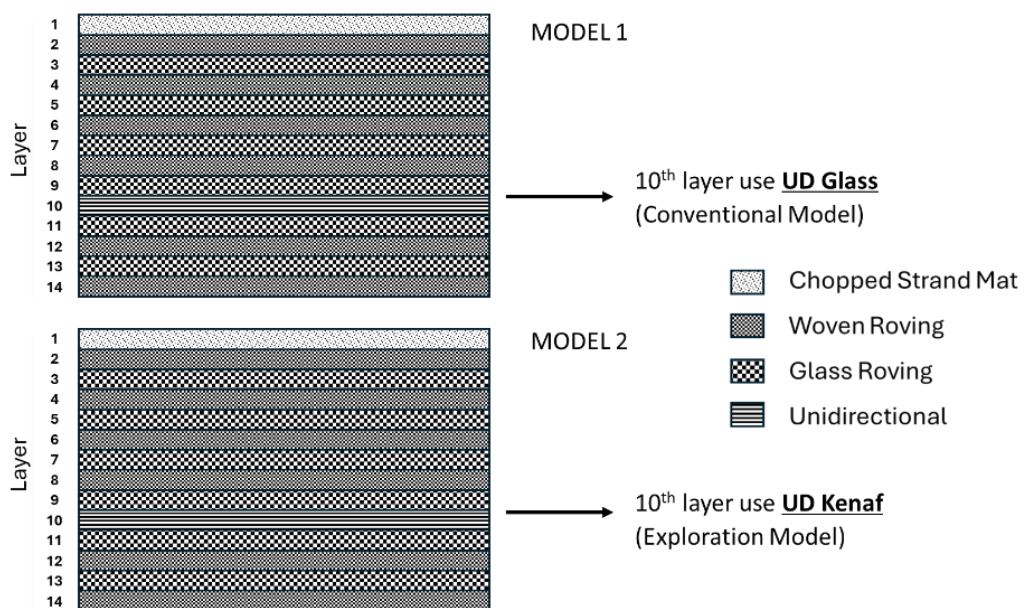


**Figure 4.** Stack up Sequence Comparison of Model 1 and Model 2

**Table 2.** Laminate Designation of Model 1 with UD Kenaf

Configuration	Code	Position of UD Kenaf in GFRP	Configuration	Code	Position of UD Kenaf in GFRP
GFRP Fan Blade	C1	-	Three layers of GR	K17	2, 4, 6
One layer of GR in	K2	2	in GFRP replaced	K18	2, 4, 8
GFRP replaced with	K3	4	with UD kenaf	K19	2, 4, 12
UD kenaf	K4	6		K20	2, 6, 8
	K5	8		K21	2, 6, 12
	K6	12		K22	2, 8, 12
Two layers of GR in	K7	2, 4		K23	4, 6, 8
GFRP replaced with	K8	2, 6		K24	4, 6, 12
UD kenaf	K9	2, 8		K25	4, 8, 12
	K10	2, 12		K26	6, 8, 12
	K11	4, 6	Four layers of GR in	K27	2, 4, 6, 8
	K12	4, 8	GFRP replaced with	K28	2, 4, 6, 12
	K13	4, 12	UD kenaf	K29	2, 4, 8, 12
	K14	6, 8		K30	2, 6, 8, 12
	K15	6, 12		K31	4, 6, 8, 12
	K16	8, 12	Five layers of GR in	K32	2, 4, 6, 8, 12
			GFRP replaced with		
			UD kenaf		

**Table 3.** Laminate designation of model 1 with UD sisal

Configuration	Code	Position of UD Sisal in GFRP	Configuration	Code	Position of UD Sisal in GFRP
GFRP Fan Blade	C1	-	Three layers of GR in	S17	2, 4, 6
One layer of GR in	S2	2	GFRP replaced with	S18	2, 4, 8
GFRP replaced with	S3	4	UD sisal	S19	2, 4, 12
UD sisal	S4	6		S20	2, 6, 8
	S5	8		S21	2, 6, 12
	S6	12		S22	2, 8, 12
Two layers of GR in	S7	2, 4		S23	4, 6, 8
GFRP replaced with	S8	2, 6		S24	4, 6, 12
UD sisal	S9	2, 8		S25	4, 8, 12
	S10	2, 12		S26	6, 8, 12
	S11	4, 6	Four layers of GR in	S27	2, 4, 6, 8
	S12	4, 8	GFRP replaced with	S28	2, 4, 6, 12
	S13	4, 12	UD sisal	S29	2, 4, 8, 12
	S14	6, 8		S30	2, 6, 8, 12
	S15	6, 12		S31	4, 6, 8, 12
	S16	8, 12	Five layers of GR in	S32	2, 4, 6, 8, 12
			GFRP replaced with		
			UD sisal		

**Table 4.** Laminate Designation of model 2 with UD kenaf

Configuration	Code	Position of UD Kenaf in GFRP	Configuration	Code	Position of UD Kenaf in GFRP
No layer of GR in GFRP replaced with UD kenaf	KK1	-	Three layers of GR in GFRP replaced with UD kenaf	KK17	2, 4, 6
One layer of GR in GFRP replaced with UD kenaf	KK2	2		KK18	2, 4, 8
	KK3	4		KK19	2, 4, 12
	KK4	6		KK20	2, 6, 8
	KK5	8		KK21	2, 6, 12
	KK6	12		KK22	2, 8, 12
	KK7	2, 4		KK23	4, 6, 8
	KK8	2, 6		KK24	4, 6, 12
	KK9	2, 8		KK25	4, 8, 12
	KK10	2, 12		KK26	6, 8, 12
	KK11	4, 6		KK27	2, 4, 6, 8
Two layers of GR in GFRP replaced with UD kenaf	KK12	4, 8	Four layers of GR in GFRP replaced with UD kenaf	KK28	2, 4, 6, 12
	KK13	4, 12		KK29	2, 4, 8, 12
	KK14	6, 8		KK30	2, 6, 8, 12
	KK15	6, 12		KK31	4, 6, 8, 12
	KK16	8, 12	Five layers of GR in GFRP replaced with UD kenaf	KK32	2, 4, 6, 8, 12

**Table 5.** Laminate designation of Model 1 with UD Sisal

Configuration	Code	Position of UD Sisal in GFRP	Configuration	Code	Position of UD Sisal in GFRP
No layer of GR in GFRP replaced with UD sisal	KK1	-	Three layers of GR in GFRP replaced with UD sisal	KS17	2, 4, 6
One layer of GR in GFRP replaced with UD sisal	KS2	2		KS18	2, 4, 8
	KS3	4		KS19	2, 4, 12
	KS4	6		KS20	2, 6, 8
	KS5	8		KS21	2, 6, 12
	KS6	12		KS22	2, 8, 12
Two layers of GR in GFRP replaced with UD sisal	KS7	2, 4		KS23	4, 6, 8
	KS8	2, 6		KS24	4, 6, 12
	KS9	2, 8		KS25	4, 8, 12
	KS10	2, 12		KS26	6, 8, 12
	KS11	4, 6	Four layers of GR in GFRP replaced with UD sisal	KS27	2, 4, 6, 8
	KS12	4, 8		KS28	2, 4, 6, 12
	KS13	4, 12		KS29	2, 4, 8, 12
	KS14	6, 8		KS30	2, 6, 8, 12
	KS15	6, 12		KS31	4, 6, 8, 12
	KS16	8, 12	Five layers of GR in GFRP replaced with UD sisal	KS32	2, 4, 6, 8, 12



### 2.3 Verification, mesh convergence, and validation

To ensure the reliability of the simulation process, a verification step was initially conducted to evaluate the mesh quality and modeling setup. The mesh metrics were assessed using skewness and orthogonal quality values. A skewness closing to 0 and an orthogonal quality closing to 1 indicate good element shapes and acceptable mesh integrity for accurate finite element calculations. The selected tetrahedral mesh with an average element size of 1.5 mm met these criteria, confirming the appropriateness of the mesh for structural analysis.

Following verification, a mesh convergence test was performed to determine the optimal element size that balanced accuracy and computational efficiency. Simulations were run using mesh sizes ranging from 5 mm to 1 mm. Table 6 summarizes the number of elements and corresponding maximum tensile stresses obtained. It was observed that stress values began to stabilize when the mesh size reached 1.5 mm, with only a negligible deviation ( $<0.04\%$ ) compared to the finest mesh (1 mm). This convergence behavior is further illustrated in Figure 5, where the stress response plateaus as the number of elements exceeded 30,000. Therefore, a mesh size of 1.5 mm with approximately 33,800 elements per model was adopted for subsequent simulations. To validate the simulation outcomes, the displacement magnitude applied in the tensile simulation was derived from the experimental failure data of the baseline GFRP specimen (C1) as reported in [2]. This displacement value was uniformly applied across all hybrid configurations to ensure consistent loading conditions for comparative analysis. Figure 6 illustrates the stress–strain response of the baseline GFRP specimen compared to experimental measurements. The simulated results fell within acceptable ranges of experimental findings reported in the literature, thereby reinforcing the validity and physical relevance of the simulation framework.

**Table 6.** Mesh convergence study on mesh size, number of nodes and elements, and resulting tensile stress

Mesh Size (mm)	Number of Nodes	Number of Elements	Stress (MPa)
5	5628	990	379.51
2	61848	13230	384.58
1.6	123000	27189	385.05
1.5	151409	33800	385.29
1	441810	101906	385.43

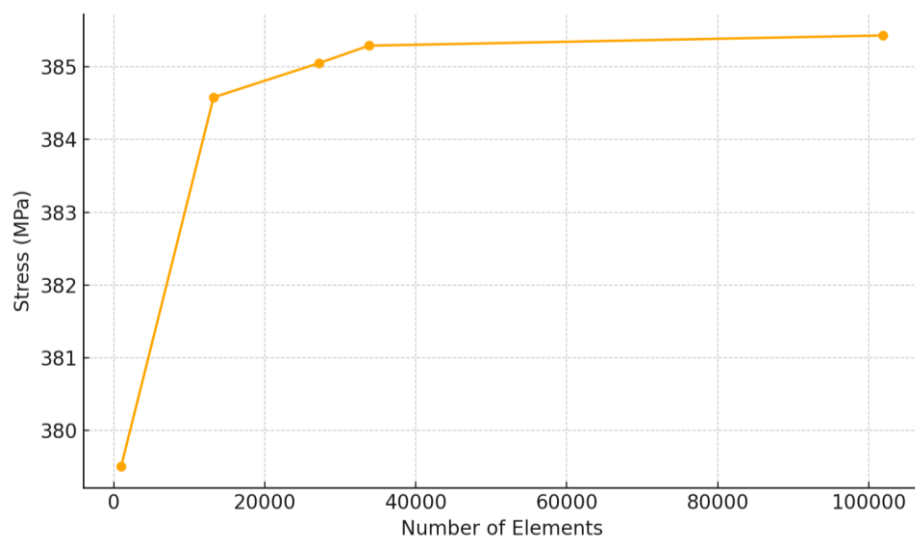


**Figure 5.** Mesh convergence curve: tensile stress vs number of elements

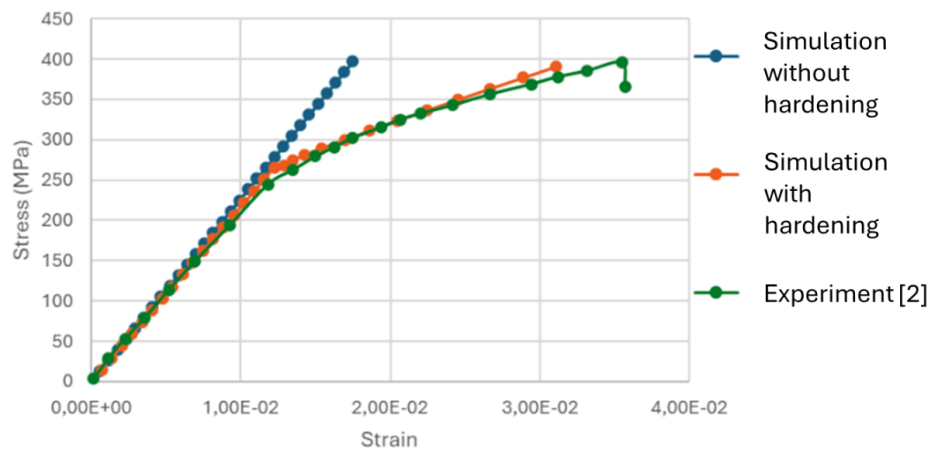


**Figure 6.** Stress–strain curves of baseline GFRP specimen (C1): comparison between experimental data and simulation results with and without bilinear isotropic hardening

### 3. Results and discussion

#### 3.1 Tensile test simulation results

Figure 7 shows the stress distribution resulted from the finite element simulation on specimen K2, in which the 2nd layer of the laminate was replaced with unidirectional (UD) kenaf fiber. The simulation applied a remote displacement equivalent to the failure displacement of the baseline specimen (C1) using conventional GFRP material. The maximum normal tensile stress observed was 451.11 MPa, occurring in the narrow-gauge section of the specimen, which was consistent with the region of highest stress concentration during tensile loading. This value reflects the ability of the K2 configuration to withstand significant axial stress. In contrast, the minimum stress located near the support boundary area, possibly due to constraint effects.

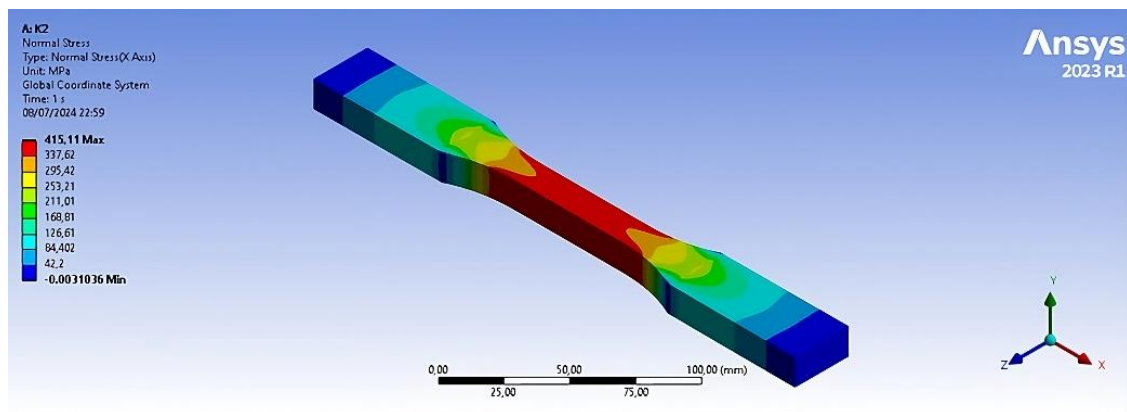
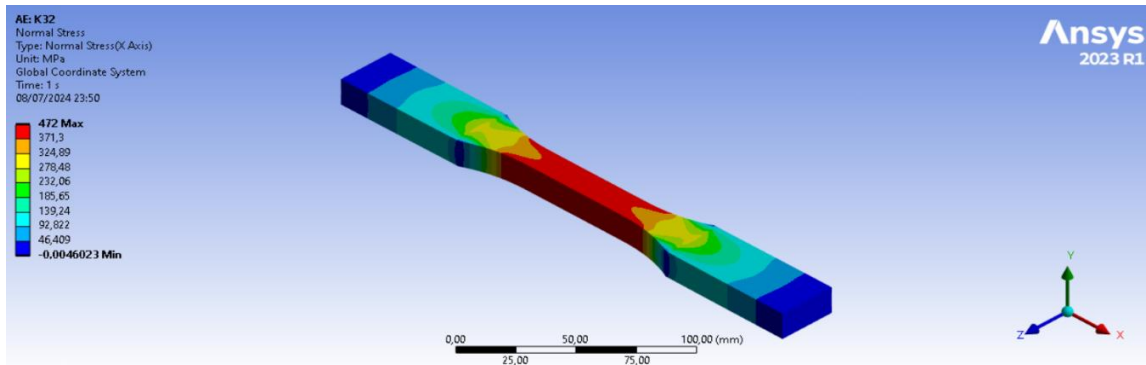


**Figure 7.** Tensile Stress Developed in K2 from Finite Element Analysis by Applying Failure Load of C1

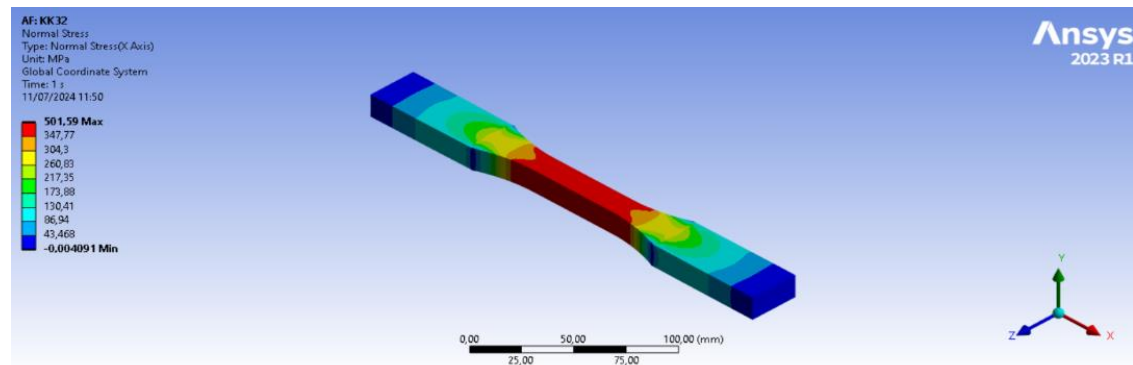
Figure 8 presents the normal stress distribution along the gauge section of two hybrid composite specimens, K32 and KK32, under tensile loading simulated using finite element analysis (FEA). Both configurations incorporate unidirectional (UD) kenaf fibers as partial replacements for glass fibers in specific laminate layers. The purpose of this comparison is to visualize the influence of different kenaf substitution strategies on stress concentration, distribution, and tensile performance. The simulation results revealed notable differences in the maximum tensile stress developed between the two configurations. In Model K32, five Glass Roving (GR) layers (2nd, 4th, 6th, 8th, and 12th) were replaced with UD kenaf, while the 10th layer remained as UD glass. This



model recorded a maximum tensile stress of 472.0 MPa. In contrast, Model KK32 not only replaced the same five GR layers but also substituted the 10th layer with UD kenaf, resulting in a higher maximum tensile stress of 507.59 MPa.



(a)



(b)

**Figure 8.** Stress distribution from tensile simulation of hybrid composite specimens: (a) K32 – five GR layers replaced with UD kenaf; (b) KK32 – five GR layers and the 10th layer replaced with UD kenaf

This increase of approximately 7.5% suggests that adding kenaf reinforcement at the structural core enhances the overall load-bearing capacity of the composite. The 10th layer, being centrally located in the laminate stack, plays a critical role in resisting axial loads; thus, replacing it with a high-performance natural fiber like kenaf can significantly impact tensile response. Additionally, kenaf's relatively high stiffness and better fiber alignment characteristics may contribute to this improved performance. The results of the maximum stress and Young's Modulus of Model 1 with the replacement of GR with UD kenaf are shown in Figure 9(a). Overall, K32 reached the highest maximum stress and Young's Modulus values, which were 472 MPa and 26.6 GPa, respectively. K32 involved replacing five layers of GR with unidirectional (UD) kenaf, specifically in the 2nd, 4th, 6th, 8th, and 12th layers.

Conversely, material with the lowest maximum stress and Young's Modulus occurred in C1 (Figure 9(a)), where there was no replacement of GR material with UD kenaf. This indicates that UD kenaf can enhance the maximum stress and Young's Modulus in GFRP materials compared to the previous use of Glass Roving (GR). Figure 9(a) indicates an increase in maximum stress and elastic modulus of the composite with the increasing number of unidirectional (UD) kenaf layers replacing Glass Roving (GR). This improvement is evident through the increase in the average maximum stress in each test group. The analysis results demonstrate that kenaf possesses superior natural mechanical

properties compared to GR, which significantly contributes to the increase in the average maximum stress and elastic modulus in the composite material.

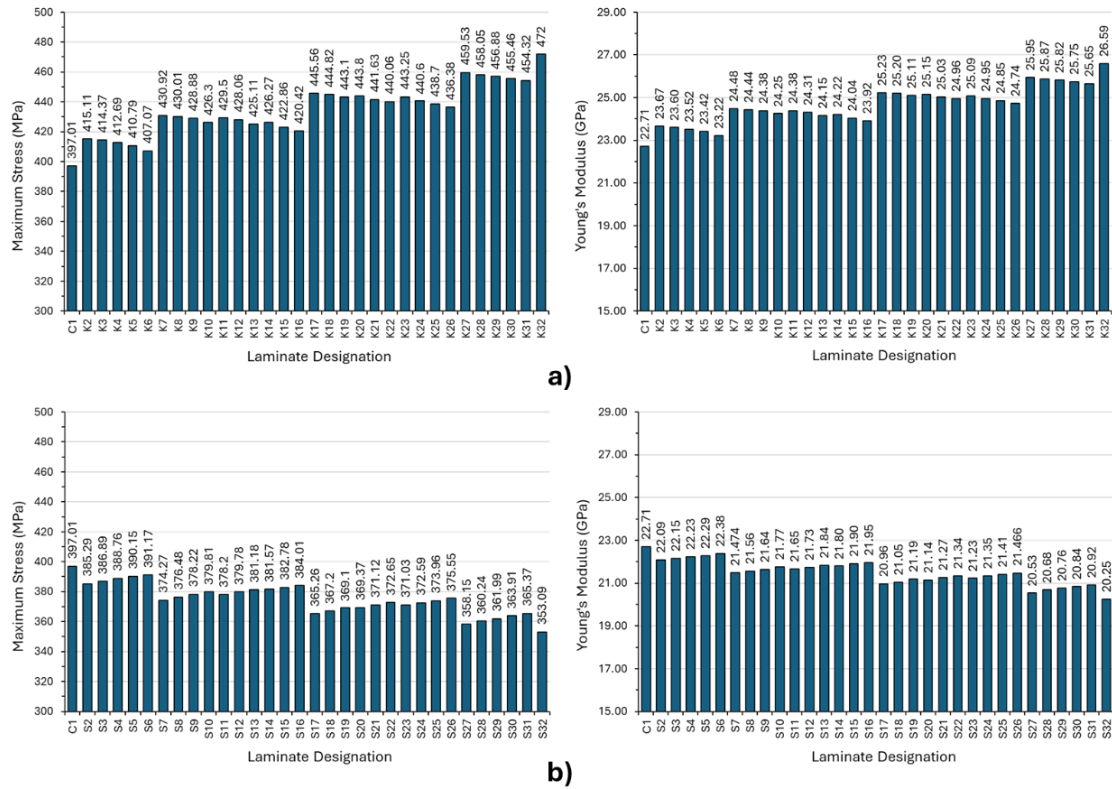


**Figure 9.** Tensile Properties Comparison of Model 1 with a) UD Kenaf; b) UD Sisal

Compared to when GR was replaced by UD sisal (Figure 9(b)), C1, which did not replace Glass Roving (GR) with Unidirectional (UD) sisal, showed the highest values for maximum stress and Young's Modulus at 397.01 MPa and 22.71 GPa, respectively. Conversely, S32, which replaced five layers of GR with UD sisal, presented the lowest values for maximum stress and Young's Modulus, at 353.09 MPa and 20.25 GPa, respectively. This result indicates that UD sisal is less effective in replacing GR in GFRP materials. From Table 3, increasing the amount of UD sisal as a replacement for GR decreases the maximum stress and Young's Modulus of the GFRP material, as indicated by the reduction in the average elastic modulus in each group. The decline in performance is due to sisal fiber inferior mechanical properties compared to GR.

The results of the tensile test of Model 2 with the replacement of GR with UD kenaf are presented in Figure 10(a). KK32 shows the best performance, with a maximum stress of 460.06 MPa and Young's modulus of 25.966 GPa. KK32 involved replacing UD Glass with UD Kenaf and substituting five layers of GR with UD Kenaf. These results indicate that UD Kenaf can enhance the tensile properties of GFRP composite materials. Compared to C1, which did not contain natural fibers, KK32 offered a 15.88% increase in maximum stress and a 14.34% increase in elastic modulus. On the other hand, KK1, which only replaced UD Glass with UD Kenaf without replacing the GR material, showed the lowest maximum stress and elastic modulus, at 386.42 MPa and 22.146 GPa, respectively. Compared to C1, KK1 showed a decrease in maximum stress by 2.67% and a decrease in elastic modulus by 2.48%. Further analysis indicates that C1 has mechanical properties comparable to KK6, which contains two layers of natural fiber. Adding a certain amount of natural fiber can achieve mechanical properties equivalent to composites without natural fiber. From Figure 10(a), it can be observed that the graph follows the same trend as in Model 1, where

the more GR layers are replaced with UD kenaf, the higher the maximum stress and Young's modulus of the material tend to be.

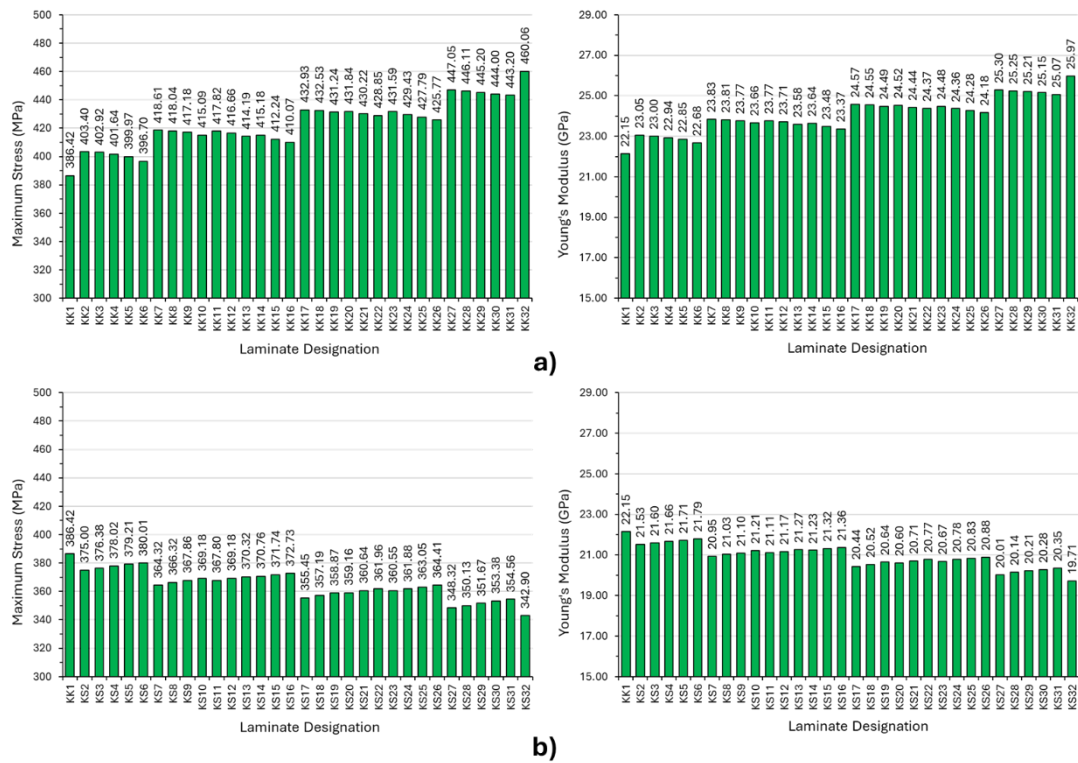


**Figure 10.** Tensile Properties Comparison of Model 2 with a) UD Kenaf; b) UD Sisal

From Figure 10(b), KK1, which only replaced UD Glass with UD Kenaf without substituting GR with UD Sisal, exhibited the highest maximum stress and Young's modulus, at 386.42 MPa and 22.146 GPa, respectively. On the other hand, the lowest maximum stress and elastic modulus were found in KS32, which recorded 342.9 MPa and 19.715 GPa, respectively. KS32 replaced UD Glass with UD Kenaf and substituted five layers of GR with UD Sisal. The reduction between KS32 and C1 was 13.63% for maximum stress and 13.2% for the elastic modulus. The tensile properties of material in Model 2 showed a decrease of 2.5% to 3% compared to Model 1. Despite this decrease, it is seen as a positive outcome as it allowed for a higher proportion of natural fibers in the material and a decrease in the use of glass fibers without significantly compromising tensile strength. This reduction is due to the differing mechanical properties between glass fibers and kenaf fibers. The relatively small decrease indicates that kenaf fibers can be a viable and more sustainable alternative to glass fibers.

### 3.2 Stress distribution analysis

In Model 1, the 10th layer used UD Glass material with a higher Young's Modulus compared to GR, CSM, and WR materials. UD glass allowed the layer to endure more stress (Figure 11 (a)). This layer served as the primary strength source in the GFRP composite material. In Model 2, the UD Glass material in the 10th layer was substituted with UD Kenaf, leveraging the superior mechanical properties of kenaf fibers. Figure 11(b) depicts the GFRP material with UD Kenaf (KK1) replacing UD Glass. In the 10th layer, UD Kenaf experienced lower stress compared to GFRP without natural fiber substitution (C1).

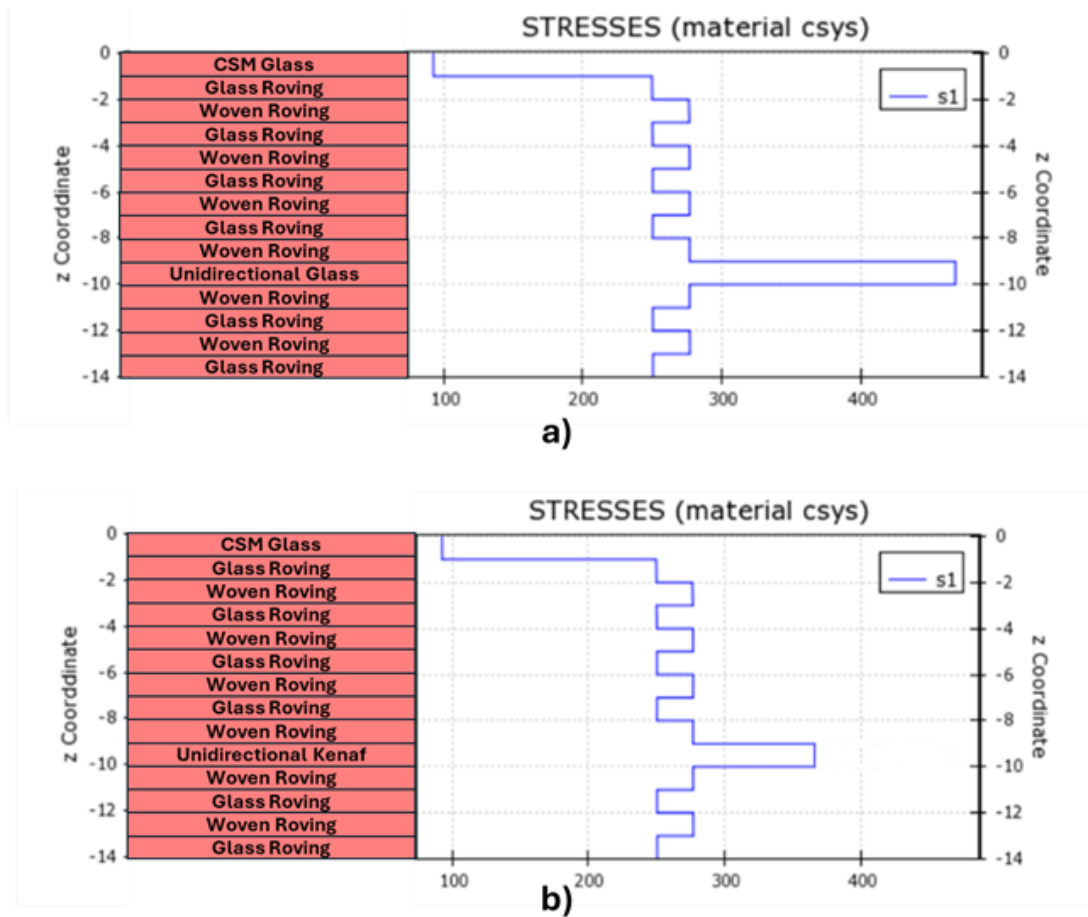


**Figure 11.** Stress Distribution of GFRP when the 10th Layer Uses a) UD Glass (C1); b) UD Kenaf (K26)

Figure 12(a) shows that Model 2 in which GR was replaced with UD Sisal in layer two experienced lower stress compared to UD Kenaf (Figure 12(b)). The substitution of GR material with UD Sisal affected the stress distribution within the GFRP composite, leading to an uneven stress distribution. The lower stress observed in UD Sisal resulted in an overall reduction in the material's tensile properties, unlike when UD Kenaf was used as a replacement material, which enhanced the material's overall tensile properties. When one layer of GR was replaced with UD Sisal in Model 2, there was an average stress reduction of 4.86% down to 377.24 MPa, compared to C1. In contrast, when one layer of GR was replaced with UD Kenaf in Model 2, there was an average stress increase of 1% up to 400.93 MPa. The more GR layers are replaced with UD Sisal, the more layers experience low stress, leading to a reduction in material maximum stress. The highest reduction occurred in KS32, with a stress value of 342.9 MPa. Conversely, the more GR layers replaced with UD Kenaf, the more layers experience high stress, leading to an increase in material maximum stress. The highest increase was in KK32, with a stress value of 460.06 MPa. These findings indicate that kenaf fibers serve as a viable alternative to synthetic fibers, offering superior biodegradability and high stiffness [26]. The superior tensile performance observed in UD kenaf compared to UD sisal can be attributed to the intrinsic material properties of the fibers. Kenaf fibers generally possess higher tensile strength and stiffness than sisal. Additionally, kenaf exhibits a more uniform fiber structure, which contributes to better stress distribution and load transfer within the composite.

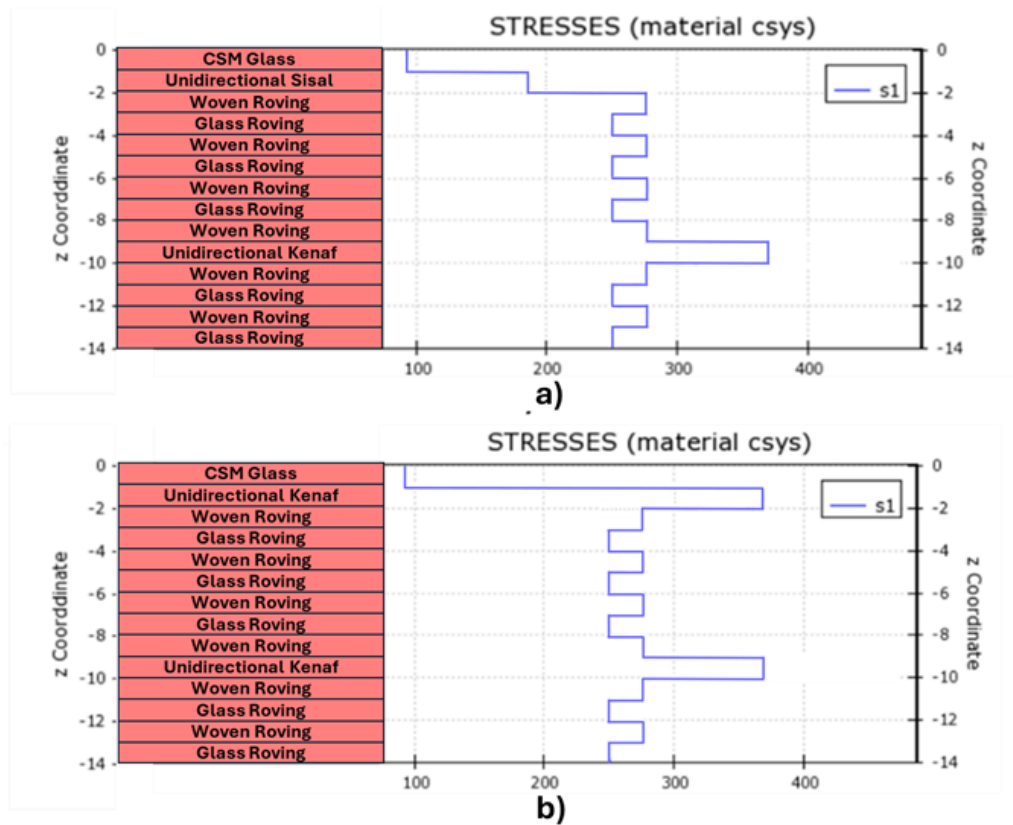


**Figure 12.** Stress Distribution of Model 2 when 1 GR Layer is Replaced with a) UD Sisal (KS2); b) UD Kenaf (KK2)

### 3.3 Correlation analysis

The results of the correlation analysis, highlighting the relationship between the position of replaced GR layers and the mechanical properties of the material, are presented in Table 7 and Table 8.

**Table 7.** Correlation Test Result of Model 1

Variable 1	Variable 2	Correlation Coefficient	
		UD Kenaf	UD Sisal
Maximum Stress	Layer 2	0.525	-0.594
	Layer 4	0.498	-0.519
	Layer 6	0.451	-0.426
	Layer 8	0.405	-0.349
	Layer 12	0.329	-0.272
Young's Modulus	Layer 2	0.538	-0.559
	Layer 4	0.491	-0.481
	Layer 6	0.446	-0.409
	Layer 8	0.404	-0.341
	Layer 12	0.326	-0.221

When GR material was replaced with UD Kenaf in GFRP composite material, the correlation coefficient showed a positive value, indicating that this substitution enhances the maximum stress and elastic modulus of the composite. However, when GR material was replaced with UD Sisal, the correlation coefficient was negative, indicating a reduction in the composite material's properties. Both Table 7 and Table 8 show that the replacement in the second layer got the highest correlation coefficient, meaning that the substitution in the second layer significantly affected the

material's maximum stress and elastic modulus compared to other positions. Conversely, the replacement in the twelfth layer showed the lowest correlation coefficient, indicating that substitution at this position does not significantly affect the elastic modulus and maximum stress.

**Table 8.** Correlation test result of model 2

Variable 1	Variable 2	Correlation Coefficient	
		UD Kenaf	UD Sisal
Maximum Stress	Layer 2	0.509	-0.577
	Layer 4	0.491	-0.513
	Layer 6	0.452	-0.429
	Layer 8	0.414	-0.361
	Layer 12	0.351	-0.295
Young's Modulus	Layer 2	0.522	-0.563
	Layer 4	0.484	-0.501
	Layer 6	0.448	-0.443
	Layer 8	0.412	-0.389
	Layer 12	0.347	-0.292

### 3.4 Discussion

This study investigates the impact of replacing glass fiber with natural fiber on the tensile properties of composite materials, focusing on maximum stress and Young's modulus. The findings confirm that kenaf fiber are promising alternatives to glass fiber due to their biodegradability and high stiffness. Additionally, the critical influence of stacking sequence and reinforcement layering on tensile performance aligns with the improved results observed when kenaf was strategically placed [27]. Supporting this, optimized stacking sequences in hybrid fiber laminates enhance both tensile and flexural strengths [28]. Furthermore, each layer experiences different stress levels, underlining the importance of layer-specific reinforcement in mechanical optimization [29]. These insights reinforce the potential of hybrid material configurations to achieve environmentally friendly composites without sacrificing mechanical performance, offering practical applications in sustainable design and manufacturing.

Despite the promising results of hybrid natural fiber composites, several challenges remain in scaling up their production for industrial applications. One key issue is the variability in the quality and mechanical properties of natural fibers, which are influenced by factors such as harvesting time, geographic origin, and processing methods. This inconsistency can affect composite performance and complicate quality control. Additionally, natural fibers are inherently hygroscopic, leading to moisture absorption that may compromise interfacial bonding and long-term durability. Another challenge is achieving strong and stable interfacial adhesion between natural fibers and polymer matrices, which often requires surface treatments or coupling agents. Finally, the fabrication process must be optimized to ensure uniform fiber dispersion and reproducibility in large-scale production. Addressing these challenges is critical to realizing the practical potential of natural fiber-reinforced hybrid composites in structural and functional components.

From an environmental perspective, incorporating natural fibers such as kenaf and sisal into GFRP composites presents clear advantages in terms of biodegradability and reduced carbon footprint. However, these environmental benefits are accompanied by certain trade-offs. Natural fibers are generally more susceptible to moisture uptake, UV degradation, and microbial attack, which may limit the long-term performance of the composites, especially under outdoor or marine conditions. These concerns raise questions on the durability and service life of such materials in harsh environments. To mitigate these risks, various surface treatments (e.g., alkali treatment, silane



coupling agents) and protective coatings can be employed to enhance moisture resistance and interfacial bonding. Such approaches are essential to extend the usability of hybrid composites while maintaining their environmental advantages.

#### 4. Conclusion

The study concludes that replacing glass roving (GR) with unidirectional (UD) Kenaf significantly improves the tensile properties of the GFRP material in fan blades. In Model 1, all variations of Kenaf showed an increase in maximum stress by up to 18.89% and Young's Modulus by up to 17.08% compared to the original GFRP (C1). Model 2 also produced positive results, with all variations, except KK1 showing improved tensile properties compared to the original GFRP. On the other hand, replacing Glass Roving with UD Sisal reduced the tensile properties of the GFRP material in both models, with a reduction in maximum stress by up to 13.63% and Young's Modulus by up to 13.18% in Model 2. Model 2, with variations in the position of UD Kenaf, was identified as the best material combination as it maximizes the amount of natural fiber without reducing the maximum stress and Young's Modulus of the original GFRP material. Overall, the variations KK2-KK32 are recommended as the best options. The use of UD Kenaf in the second layer demonstrated a significant improvement in tensile properties, making it a strategic choice for enhancing the tensile properties of GFRP composites. Conversely, using UD Sisal, especially in the second layer, reduces the material's tensile properties and should be limited to non-critical layers that are not directly affected by tensile loads. This finding has practical implications for the design and manufacture of fan blades, as it suggests a potential method for enhancing their performance.

#### Author's declaration

#### Author contribution

**Alief Wikarta:** Conceptualization, designed, and developed the research, contributed to the refinement of the research, assisted in writing and proofreading the manuscript; **Chandya Andikusuma:** Conceptualization, co-developed and designed the research, collected and analyzed data, drafted the manuscript; **Julendra Bambang Ariatedja:** Assisted in refining and clarifying the methodology and results, assisted in drafting the manuscript; **I Made Londen Batan:** Assisted in refining methodology and results. **Femiana Gapsari:** Assisted in drafting the manuscript; **Sze Wei Khoo:** numerical calculations and review and editing.

#### Funding statement

This study was funded by the Research, Innovation, and Entrepreneurship grant under the Higher Education for Technology and Innovation (HETI) Project, ADB Loan No. 4110-INO, through the Innovative Entrepreneurship (IE) scheme at Institut Teknologi Sepuluh Nopember, based on contract number 0086/01.PKS/PPK-HETI/ITS/2024.

#### Data Availability

Data will be made available on request.

#### Acknowledgement

The authors express their sincere gratitude to all individuals for their invaluable support and assistance during this research.

## Competing interest

The authors declare no competing interest.

## Ethical clearance

This research does not involve humans or animals as subjects, so an ethical document is not required.

## AI statement

This article is the author's original work, written from original research, and no sections or figures are generated by AI. The language use of this article has been checked and verified by an English language expert.

## Publisher's and Journal's note

Universitas Negeri Padang as the publisher, and Editor of Teknomekanik state that there is no conflict of interest towards this article publication.

## References

- [1] M. K. Buragohain, *Composite Structures*. CRC Press, 2017.  
<https://doi.org/10.1201/9781315268057>
- [2] V. S. Chinta, P. Ravinder Reddy, and K. E. Prasad, "The effect of stacking sequence on the tensile properties of jute fibre reinforced hybrid composite material for axial flow fan blades: An experimental and finite element investigation," *Mater Today Proc*, vol. 59, pp. 747–755, 2022, <https://doi.org/10.1016/j.matpr.2021.12.500>
- [3] C. I. Morăraș, V. Goanță, D. Husaru, B. Istrate, P. D. Bârsănescu, and C. Munteanu, "Analysis of the Effect of Fiber Orientation on Mechanical and Elastic Characteristics at Axial Stresses of GFRP Used in Wind Turbine Blades," *Polymers (Basel)*, vol. 15, no. 4, p. 861, Feb. 2023, <https://doi.org/10.3390/polym15040861>
- [4] H. Xin, A. S. Mosallam, Y. Liu, C. Wang, and J. He, "Experimental and numerical investigation on assessing local bearing behavior of a pultruded GFRP bridge deck," *Compos Struct*, vol. 204, pp. 712–730, Nov. 2018, <https://doi.org/10.1016/j.compstruct.2018.07.082>
- [5] S. Duan, X. Yang, Y. Tao, F. Mo, Z. Xiao, and K. Wei, "Experimental and numerical investigation of Long Glass Fiber Reinforced Polypropylene composite and application in automobile components," *Transport*, pp. 1–9, May 2017, <https://doi.org/10.3846/16484142.2017.1323231>
- [6] S.-C. Shi *et al.*, "Rice straw-derived chitosan-enhanced plasticizers as biologically and environmentally friendly alternatives for sustainable materials," *Int J Biol Macromol*, vol. 264, p. 130547, Apr. 2024, <https://doi.org/10.1016/j.ijbiomac.2024.130547>
- [7] S.-C. Shi, X.-N. Tsai, and D. Rahmadiawan, "Enhancing the tribological performance of hydroxypropyl methylcellulose composite coatings through nano-sized metal and oxide additives: A comparative study," *Surf Coat Technol*, vol. 483, p. 130712, May 2024, <https://doi.org/10.1016/j.surfcoat.2024.130712>
- [8] M. R. Sanjay, P. Madhu, M. Jawaid, P. Senthamaraiannan, S. Senthil, and S. Pradeep, "Characterization and properties of natural fiber polymer composites: A comprehensive review," *J Clean Prod*, vol. 172, pp. 566–581, Jan. 2018, <https://doi.org/10.1016/j.jclepro.2017.10.101>

- [9] O. Faruk, A. K. Bledzki, H.-P. Fink, and M. Sain, "Biocomposites reinforced with natural fibers: 2000–2010," *Prog Polym Sci*, vol. 37, no. 11, pp. 1552–1596, Nov. 2012, <https://doi.org/10.1016/j.progpolymsci.2012.04.003>
- [10] Y. G. Thyavihalli Girijappa, S. Mavinkere Rangappa, J. Parameswaranpillai, and S. Siengchin, "Natural Fibers as Sustainable and Renewable Resource for Development of Eco-Friendly Composites: A Comprehensive Review," *Front Mater*, vol. 6, Sep. 2019, <https://doi.org/10.3389/fmats.2019.00226>
- [11] A. Gholampour and T. Ozbakkaloglu, "A review of natural fiber composites: properties, modification and processing techniques, characterization, applications," *J Mater Sci*, vol. 55, no. 3, pp. 829–892, Jan. 2020, <https://doi.org/10.1007/s10853-019-03990-y>
- [12] K. Senthilkumar *et al.*, "Mechanical properties evaluation of sisal fibre reinforced polymer composites: A review," *Constr Build Mater*, vol. 174, pp. 713–729, Jun. 2018, <https://doi.org/10.1016/j.conbuildmat.2018.04.143>
- [13] N. R. J. Hynes *et al.*, "Effect of stacking sequence of fibre metal laminates with carbon fibre reinforced composites on mechanical attributes: Numerical simulations and experimental validation," *Compos Sci Technol*, vol. 221, p. 109303, Apr. 2022, <https://doi.org/10.1016/j.compscitech.2022.109303>
- [14] T. Mishra, P. Mandal, A. K. Rout, and D. Sahoo, "A state-of-the-art review on potential applications of natural fiber-reinforced polymer composite filled with inorganic nanoparticle," *Composites Part C: Open Access*, vol. 9, p. 100298, Oct. 2022, <https://doi.org/10.1016/j.jcomc.2022.100298>
- [15] R. M. Abhilash, G. S. Venkatesh, and S. S. Chauhan, "Micromechanical modeling of bamboo short fiber reinforced polypropylene composites," *Multiscale and Multidisciplinary Modeling, Experiments and Design*, vol. 4, no. 1, pp. 25–40, Mar. 2021, <https://doi.org/10.1007/s41939-020-00081-3>
- [16] M. Rouway *et al.*, "Prediction of Mechanical Performance of Natural Fibers Polypropylene Composites: a Comparison Study," *IOP Conf Ser Mater Sci Eng*, vol. 948, no. 1, p. 012031, Nov. 2020, <https://doi.org/10.1088/1757-899X/948/1/012031>
- [17] Z. I. Makruf, W. Afnison, and B. Rahim, "A Study on the utilization of areca nut husk fiber as a natural fibre reinforcement in composite applications: A systematic literature review," *Journal of Engineering Researcher and Lecturer*, vol. 3, no. 1, pp. 18–28, Apr. 2024, <https://doi.org/10.58712/jerel.v3i1.123>
- [18] G. R. Kumar, R. Vijayanandh, M. S. Kumar, and S. S. Kumar, "Experimental testing and numerical simulation on natural composite for aerospace applications," 2018, p. 090045. <https://doi.org/10.1063/1.5032892>
- [19] N. M. Nurazzi *et al.*, "A Review on Mechanical Performance of Hybrid Natural Fiber Polymer Composites for Structural Applications," *Polymers (Basel)*, vol. 13, no. 13, p. 2170, Jun. 2021, <https://doi.org/10.3390/polym13132170>
- [20] M. A. R. Ferdian and A. Wikarta, "Mechanical Properties of the Polyester Hybrid Composite Reinforced by Fiberglass and Bamboo Blades as the Replacement Materials for 10GT Boat," 2025, pp. 259–267. [https://doi.org/10.1007/978-981-97-7898-0\\_29](https://doi.org/10.1007/978-981-97-7898-0_29)
- [21] C. Balaji Ayyanar *et al.*, "Experimental and numerical analysis of natural fillers loaded and E-glass reinforced epoxy sandwich composites," *Journal of Materials Research and Technology*, vol. 32, pp. 1235–1244, Sep. 2024, <https://doi.org/10.1016/j.jmrt.2024.07.142>
- [22] H. Ku, H. Wang, N. Pattarachaiyakoop, and M. Trada, "A review on the tensile properties of natural fiber reinforced polymer composites," *Compos B Eng*, vol. 42, no. 4, pp. 856–873, Jun. 2011, <https://doi.org/10.1016/j.compositesb.2011.01.010>
- [23] K. Yorseng, S. M. Rangappa, H. Pulikkalparambil, S. Siengchin, and J. Parameswaranpillai, "Accelerated weathering studies of kenaf/sisal fiber fabric reinforced fully biobased hybrid bioepoxy composites for semi-structural applications: Morphology, thermo-mechanical, water absorption behavior and surface hydrophobicity," *Constr Build Mater*, vol. 235, p. 117464, Feb. 2020, <https://doi.org/10.1016/j.conbuildmat.2019.117464>

- [24] J. Naveen, M. Jawaid, P. Amuthakkannan, and M. Chandrasekar, "Mechanical and physical properties of sisal and hybrid sisal fiber-reinforced polymer composites," in *Mechanical and Physical Testing of Biocomposites, Fibre-Reinforced Composites and Hybrid Composites*, Elsevier, 2019, pp. 427–440. <https://doi.org/10.1016/B978-0-08-102292-4.00021-7>
- [25] A. Manral and P. K. Bajpai, "Analysis of properties on chemical treatment of kenaf fibers," *Mater Today Proc*, vol. 40, pp. S35–S38, 2021, <https://doi.org/10.1016/j.matpr.2020.03.266>
- [26] Y. Wu, C. Xia, L. Cai, A. C. Garcia, and S. Q. Shi, "Development of natural fiber-reinforced composite with comparable mechanical properties and reduced energy consumption and environmental impacts for replacing automotive glass-fiber sheet molding compound," *J Clean Prod*, vol. 184, pp. 92–100, May 2018, <https://doi.org/10.1016/j.jclepro.2018.02.257>
- [27] N. A. Nik Ismail, M. Nazrul Roslan, A. E. Ismail, and M. Yazid Yahaya, "Influence of reinforcement stacking sequence and mesh size on the tensile performance of novel hybrid bamboo fiber/aluminium mesh reinforced polymer composites," *Mater Today Proc*, Mar. 2023, <https://doi.org/10.1016/j.matpr.2023.03.315>
- [28] Y. Wang, W. Sun, and L. Cao, "Tensile and flexural mechanical attributes of hybrid carbon/basalt fiber metal laminates under various hybridization and stacking sequences," *Compos Part A Appl Sci Manuf*, vol. 177, p. 107942, Feb. 2024, <https://doi.org/10.1016/j.compositesa.2023.107942>
- [29] K. Anam, A. Purnowidodo, B. Ananta, and P. K. A. V. Kumar, "The Effect of Load Steps and Initial Crack Length on Stress Distribution of Fiber Metal Laminates," *Mechanics Exploration and Material Innovation*, vol. 1, no. 2, pp. 54–60, Apr. 2024, <https://doi.org/10.21776/ub.memi.2024.001.02.3>